www.czasopisma.pan.pl PAN www.journals.pan.pl
Opto-Electronics Review 29 (2021) 59-70

PAN POLISH ACADEMY OF SCIENCES

Opto-Electronics Review

journal homepage: http://journals.pan.pl/opelre

PAPR reduction using a combination between precoding and non-linear companding techniques for ACO-OFDM-based VLC systems

N. A. Mohammed [a*], M. M. Elnabawy [b,c], A. A. M. Khalaf [b]

[a] Photonic Research Lab, Electrical Engineering Department, College of Engineering, Shaqra University, Dawadmi 11961, Kingdom of Saudi Arabia
[b] Electrical Engineering Department, Faculty of Engineering, Minia University, Minia, Egypt, P.O. Box 61111, Minia, Egypt
[c] Electronics and Communication Department, Modern Academy for Engineering and Technology, Maadi 11585, Cairo, Egypt

Article info

Article history:
Received 3 Apr. 2021
Accepted 1 Jun. 2021

Keywords:
visible light communication, light emitting diode, peak-to-average power ratio, bit error rate

Abstract

Peak-to-average power ratio reduction techniques for visible light communication broadcasting systems are designed, simulated, and evaluated in this work. The proposed techniques are based on merging non-linear companding techniques with precoding techniques. This work aims to nominate an optimum novel scheme combining the low peak-to-average power ratio with the acceptable bit error rate performance. Asymmetrically clipped optical orthogonal frequency division multiplexing with the low peak-to-average power ratio performance becomes more attractive to real-life visible light communication applications due to non-linearity elimination. The proposed schemes are compared and an optimum choice is nominated. Comparing the presented work and related literature reviews for peak-to-average power ratio reduction techniques are held to ensure the proposed schemes validity and effectiveness.

1. Introduction

Visible light communication (VLC) adopts light-emitting diodes (LEDs) to transmit data in the visible light spectrum. VLC is an efficient method for wireless data transmission in indoor environments, especially for low mobility and short-range applications [1]. These systems offer several advantages compared to radiofrequency (RF) systems, such as the lower implementation cost, free license bandwidth, which is a remarkable advantage of VLC technology, enhanced privacy, and security since light rays cannot propagate through walls [2].

Moreover, VLC has become a state of art optical communication technology. It can be considered an advanced version of free-space optical communication (FSO), especially for indoor environments. Several optoelectronic/photonic devices/platforms such as Mach Zehnder interferometer (MZI), Fiber Bragg grating (FBG), and semiconductor optical amplifiers (SOAs) began to focus and switch some of their applications to keep up with the noticeable widespread of VLC technology, especially in indoor optical communication environments [3–7].

Although photonic crystals and other all-optical devices show a promising integration ability and a remarkable power consumption performance, they suffer from complex system and structure designs compared to VLC technology [8–12].

VLC is used in many applications, including localization, high-speed video streaming, high bit-rate data broadcasting in indoor buildings, underwater data transmission. It is also preferred in the environments sensitive to electromagnetic interference (EMI) like aircraft and vehicle-to-vehicle communication systems [13–15]. VLC and dense wavelength division multiplexing are adopted in the new communication technology such as the 5G mobile communication system [3]. VLC data broadcasting in indoor buildings is a research field that easily meets illumination and communication requirements [16]. Dimming control (i.e., controlling lighting levels) while sustaining communication links is achieved using

*Corresponding author at: nazzazzz@gmail.com

https://doi.org/10.24425/opelre.2021.135829.
1896-3757/ Association of Polish Electrical Engineers (SEP) and Polish Academic of Sciences (PAS). Published by PAS

different modulation techniques. VLC modulation techniques basically fall into two main categories: single carrier modulation (SCM) and multicarrier modulation (MCM) techniques. It is noteworthy to mention that, at low operating system rates, SCM techniques such as pulse amplitude modulation (PAM), pulse width modulation (PWM), pulse position modulation (PPM), and on-off keying (OOK) are used for implementing a VLC system. However, SCM techniques are imposed to the problem of an inter-symbol interference (ISI) at higher operating bit rates [17,18]. MCM techniques with optical orthogonal frequency division multiplexing (OOFDM) as a nominated technique are introduced to overcome SCM techniques disadvantages. MCM techniques are presented as modulation techniques for the future of high-speed VLC communication systems and applications. Unfortunately, this comes at the expense of the system complexity [1,19–22].

OOFDM is thought to be an attractive modulation scheme for increasing the modulation bandwidth of LEDs. [20]. Recently, several OOFDM schemes have been proposed. Asymmetrically clipped optical OFDM (ACO-OFDM) [20], unipolar OFDM (U-OFDM) [23], and flip OFDM can achieve a better power efficiency than a traditional direct-current biassed optical orthogonal frequency division multiplexing (DCO-OFDM) at the expense of reducing half of the spectral efficiency [24–27]. Improved systems, such as enhanced unipolar OFDM (eU-OFDM) [28], spectral and energy-efficient OFDM (SEE-OFDM) [29,30], and polar OFDM (P-OFDM) [31] are added to compensate for the reduction in spectral performance. The fundamental principles of eU-OFDM and SEE-OFDM are the same. Combining different signals at the transmitter and demodulating them independently at the receiver are illustrations of these concepts. However, the spectral efficiency improvement is achieved by the increase of signal paths and system complexity. A polar coordinate transformation is used in P-OFDM to achieve the appropriate signal format for a VLC transmission in which no spectral efficiency penalty is imposed. To sum up, ACO-OFDM is a key scheme that many previous optimized schemes with enhancement features are based on. The last idea with what has been mentioned previously about ACO-OFDM advantages and the fact that it is one of the most today's practical schemes for VLC communication systems are the factors that make this work concentrate on this type in particular [32–37].

Generally, all MCM schemes face significant challenges that limit their targeted high-speed VLC communication. Peak-to-average power ratio (PAPR) and the complexity of generation/demodulation MCM signals are examples of these challenges. The most significant drawback of MCM schemes is that the signal profile contains transient peaks that appear throughout the OFDM signal, significantly contributing to PAPR [25]. PAPR occurs primarily when parallel data streams are combined to form the OFDM/OOFDM signal. As the subcarrier-modulated symbols are applied in the same step, the signal reaches its maximum power. High PAPR values are an intrinsic drawback of OFDM, resulting in non-linear signal distortions and high power requirements for the transmitter amplifier [34].

This problem origin can be illustrated in VLC: LEDs are used as transmitters, and high-power signals can easily impair them. LEDs have a narrow working voltage range, and the voltage-to-current (V-I) relationship is non-linear. LEDs non-linear V-I characteristic distorts the OFDM signal with a high PAPR. LED chips can overheat due to their high peak power. As a result, the high PAPR of the OFDM signal should be decreased until it is fed into the transmitter LEDs [38].

PAPR reduction approaches for MCM techniques can be divided into three groups based on strategy: adding signal techniques (AST), multiple signal representation (MSR) techniques, and coding techniques (CT)/precoding techniques (PCT) [39].

PAPR is reduced by AST using three major techniques: signal clipping, compressing large peaks using non-linear companding transform (NCT), and applying peak reduction signal/or stretching the constellation. These methods introduce distortion noises into the broadcast signal which cannot be eliminated. NCT is a widely used and most promising technique [40–42]. The companding function is added to the initial OOFDM signal in NCT in order to increase small signal amplitudes and compress high signal amplitudes. The signal average power can be kept constant by using the companding function. The main types of NCT are A-law, μ-law, exponential, and cos companding techniques [43–46].

MSR strategies produce alternate signals for the same signal by changing phases, amplitude, and phases or data locations. The major drawbacks of this approach include an increase in computing complexity and the need to transmit side information for the receiver which reduces bandwidth efficiency. Partial transmit sequence (PTS) and selective mapping (SLM) techniques are the two most common types of MSR [47–49].

Finally, CT can increase side information, computational complexity or operate only with a limited number of subcarriers which is inefficient for a high-speed VLC-OOFDM communication. The drawbacks of CT can be mitigated by using PCT. The famous types of PCT are Walsh–Hadamard transform (WHT), discrete cosine transform (DCT), discrete Hartley transform (DHT), and Vandermonde like matrix (VLM) transform [37,39,47,50].

Precoding methods minimize PAPR without compromising the bit error rate (BER) efficiency and they do not require side details or additional processing. Any precoding methods, such as WHT, DCT, DHT, and VLM have been investigated to reduce an OFDM signal high PAPR.

The novelty of this work lies in three main points. First, to the authors' best knowledge, it is the first time to explore the effect of applying types of the NCT (i.e., A-law and cos) on the PAPR and BER performance in a VLC based system (i.e., studied previously for RF systems), as will be discussed in section 4.1. Second, both the BER and PAPR performance will be explored using PCT (i.e., only PAPR is studied for the VLC system [51]); and this will be discussed in section 4.2. Finally, to the authors' best knowledge, it is the first time to propose using NCT combined with PCT for the ACO-OFDM-based VLC system to reduce the PAPR problem. Also, the BER performance will be evaluated. A combined analysis will be carried out in section 4.3. A comparison between all these techniques regarding PAPR and BER performance will be introduced in section 4.4.

The paper is organized as follows: section 2 describes the ACO-OFDM system model and parameters. section 3 explains PAPR reduction techniques and the proposed PAPR reduction system. The results of the simulation and the comparison between the proposed plans are discussed in section 4. A comparison between the study and related literature reviews is presented in section 5. The conclusion is drawn in section 6.

2. ACO-OFDM system model and PAPR

Figure 1 depicts a conventional IM/DD optical wireless transmission scheme using ACO-OFDM with N subcarriers. The transmitted bitstream is mapped into the complex-valued symbols $A_k, k = 0,1,\cdots,N-1$, based on the modulation scheme selected, such as quadrature amplitude modulation (QAM). OFDM subcarriers are subjected to Hermitian symmetry to ensure that time-domain signals are real-valued which means that $A_k = A^*_{N-k}, k = 1,2,\dots,N/2-1$. To ensure that the time-domain signals can be explicitly clipped at zero, only odd subcarriers are modulated. The frequency-domain ACO-OFDM signals are denoted by [52]:

$$A = [0, A_1, 0, A_3, \dots, A_{N/2-1}, 0, A^*_{N/2-1}, \dots, A^*_1]. \quad (1)$$

The inverse fast fourier transform (IFFT) yields the time-domain ACO-OFDM signal as:

$$a_{ACO,n} = \frac{1}{\sqrt{N}} \sum_{k=0}^{N-1} A_k \exp\left(j\frac{2\pi}{N}kn\right), n = 0,1,\cdots,N-1, \quad (2)$$

which follows a half-wave symmetry as:

$$a_{ACO,n} = -a_{ACO,n+N/2}, n = 0,1,\cdots,N/2-1. \quad (3)$$

As a result, the negative aspect can be clipped without losing any information:

$$\lfloor a_{ACO,n} \rfloor_c = a_{ACO,n} + i_{ACO,n} = \begin{cases} a_{ACO,n}, a_{ACO,n} \geq 0; \\ 0, \quad a_{ACO,n} \leq 0; \end{cases} \quad (4)$$

For $n = 0,1,\cdots,N-1$, where $i_{ACO,n}$ denotes the negative clipping distortion of ACO-OFDM.

Even after the IFFT operation, a cyclic prefix (CP) is appended to the beginning of each time-domain OFDM symbol to remove ISI at the receiver. The signal is then converted from parallel to serial (P/S) into a single signal stream before being clipped at zero and modulating the LEDs [32].

An avalanche photodiode (APD) detects the optical signal and converts it to an electrical signal at the receiver. It has been demonstrated in Ref. 53 that when converted to the frequency domain, the negative clipping distortion only occurs on the even subcarriers and is orthogonal to the transmitted data on the odd subcarriers. Thus, after serial-to-parallel (S/P) conversion and CP exclusion, the transmitted signal of the odd subcarriers can be retrieved using a basic FFT operation at the receiver.

The statistical relationship of the PAPR for an OOFDM signal is the maximal power to average power, which is [54]:

$$PAPR = \frac{max\left\{\left|\lfloor a_{ACO,n} \rfloor_c\right|^2\right\}}{E\left|\lfloor a_{ACO,n} \rfloor_c\right|^2}, \quad (5)$$

where $E\{.\}$ stands for the statistical expectation.

A complementary cumulative distribution function (CCDF) is often used to evaluate the output of the PAPR reduction technique. CCDF is the probability that an OOFDM signal PAPR is greater than the given threshold PAPR ($PAPR_0$), expressed as:

$$CCDF = P(PAPR > PAPR_0) = 1 - (1 - e^{-PAPR_0})^N. \quad (6)$$

3. PAPR reduction techniques and proposed model

This section is divided into three main parts. The mathematical modeling for PCT is presented in section 3.1. NCT and its inverse are given in section 3.2. The proposed VLC system that uses NCT combined with the PCT for ACO-OFDM is proposed in section 3.3.

3.1 Precoding techniques (PCT)

3.1.1 Walsh Hadamard transform (WHT)

W_N is the Hadamard matrix with elements 1 or −1. The Hadamard matrix of orders 1, 2, and 2N is computed as follows [55]:

$$W_1 = [1]\ ;\ W_2 = \frac{1}{\sqrt{2}}\begin{bmatrix} 1 & 1 \\ 1 & -1 \end{bmatrix}\ ;\ W_{2N} = \frac{1}{\sqrt{2N}}\begin{bmatrix} W_N & W_N \\ W_N & -W_N \end{bmatrix}, \quad (7)$$

where W_N is complementary of W_N.

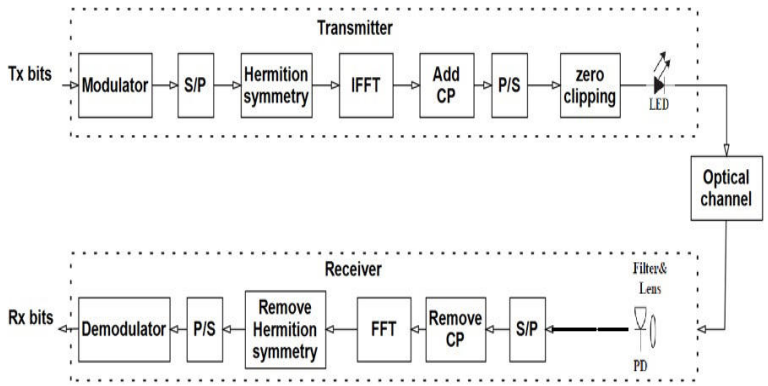

Fig. 1. Conventional ACO-OFDM-based VLC system.

3.1.2 Discrete cosine transform (DCT)

The DCT is a real transformation that involves multiplying the data by a cosine equation. The following equation [56] can be used to obtain an element of a matrix B of size N × N in the m-*th* row and n-*th* column:

$$B_{mn} = \begin{cases} \frac{1}{\sqrt{N}} & \begin{cases} m = 0 \\ 0 \le n \le N-1 \end{cases} \\ \frac{1}{\sqrt{N}} cos\left(\frac{\pi}{N}(n+0.5)m\right) & \begin{cases} 1 \le m \le N-1 \\ 0 \le n \le N-1 \end{cases} \end{cases} \quad (8)$$

3.1.3 Discrete Hartley transform (DHT)

Each element of the DHT matrix B in the m-*th* row and n-*th* column B_{mn} is defined as follows [57]:

$$B_{mn} = \frac{1}{\sqrt{N}}\left[\cos\left(\frac{2\pi}{N}mn\right) + \sin\left(\frac{2\pi}{N}mn\right)\right], \quad (9)$$

where $0 \le m, n \le N-1$.

3.1.4 Vandermonde like matrix (VLM)

The VLM transform is used before the IFFT procedure to reduce the autocorrelation of the input series, thus lowering the PAPR of the OFDM signal. VLMs can be generated in two forms [47]:

$$B_{mn}^{(1)} = \sqrt{\frac{2}{N+1}}\cos\left(\frac{2}{N+1}(m-1)(n-1)\right) \quad (10)$$

$$B_{mn}^{(2)} = \sqrt{\frac{2}{N+1}}\cos\left(\frac{2}{N+1}(m-1)(n-1/2)\right) \quad (11)$$

where $0 \le m, n \le N-1$.

Both matrices described above have the same PAPR reduction efficiency. As a result, only the first kind of VLM transform has been used in the simulation.

3.2 Non-linear companding techniques (NCT)

3.2.1 μ-law companding transform

The compressor characteristic in the μ-law companding is piecewise, consisting of a linear segment for low-level inputs and a logarithmic segment for high-level inputs. The signal is compressed at the transmitter and reconstructed at the receiver using the subsequent expanding processing. Reference 58 has the compressing:

$$A_c(n) = V_{max}\frac{\log(1+\mu|\bar{A}(n)|/V_{max})}{\log(1+\mu)}\text{sgn}[\bar{A}(n)], \quad (12)$$

where $V_{max} = max(\bar{A}(n))$, $n = 0,1,\dots,N-1$. μ is a companding parameter that can be adjusted to control the degree of the PAPR reduction for OFDM signals. $A_c(n)$ is the sample that has been combined. $\bar{A}(n)$ is the original sample. The method of expansion is simply the opposite to Eq. (12), as shown below:

$$\hat{\bar{A}}(n) = \frac{V_{max}}{\mu}\left[\exp\left[\frac{|A_c(n)|\ln[1+\mu]}{V_{max}}\right]\right]\text{sgn}[A_c(n)], \quad (13)$$

where $\hat{\bar{A}}(n)$ is the sample that was calculated after expansion.

3.2.2 A-law companding transform

The compressor characteristic is piecewise in this companding form, consisting of a linear segment for low-level inputs and a logarithmic segment for high-level inputs. This strategy has the potential to reduce the PAPR, which is the primary drawback of OFDM [59].

$$y(x) = \begin{cases} y_{max}\frac{A\frac{|x|}{x_{max}}}{(1+A)}\text{sgn}(x), & 0 < \frac{|x|}{x_{max}} \le \frac{1}{A} \\ y_{max}\frac{\left[1+\log_e\left[A\frac{|x|}{x_{max}}\right]\right]}{(1+\log_e A)}\text{sgn}(x), & \frac{1}{A} < \frac{|x|}{x_{max}} \le 1 \end{cases} \quad (14)$$

where x: input signal, y: output signal, and A is the companding factor.

3.2.3 Cos companding

The signal is compressed at the transmitter and reconstructed at the receiver using the subsequent expanding processing. Reference 60 gives the compressing function:

$$h(x) = \text{sgn}(x)\sqrt[y]{\alpha\left[1-\cos\left(-\frac{|x|}{\sigma}\right)\right]}, \quad (15)$$

where $h(x)$: compressed signal, y: compression parameter, $\text{sgn}(x)$: sign function, and σ is the standard deviation of the instantaneous input signal $|x|$.

The inverse function $h(x)$ is used in the decompanding procedure at the receiver side:

$$h^{-1}(x) = \text{sgn}(x)\left|-\sigma\text{acos}\left(1-\frac{|x|^{\frac{2}{y}}}{\alpha}\right)\right|. \quad (16)$$

The average power of output signals is determined by the positive constant α to maintain the same average power ratio of the input and output signals.

$$\alpha = \left(\frac{E[|x|^2]}{E\left[\sqrt[d]{\left[1-\exp\left(-\frac{|x|}{\sigma}\right)\right]^2}\right]}\right)^{\frac{y}{2}}, \quad (17)$$

where d denotes the companding scheme degree.

3.3 Proposed PAPR reduction system

Figure 2 represents the proposed combined precoding and companding techniques for the ACO-OFDM-based VLC system. It differs from the conventional one (i.e., Fig. 1). In the proposed units (named for abbreviations 1 to 4) the techniques are indicated by the yellow color as shown in Fig. 2. The mathematical description and rules for units 1 and 4 were previously only discussed in section 3.1. While units 2 and 3 are found in section 3.2.

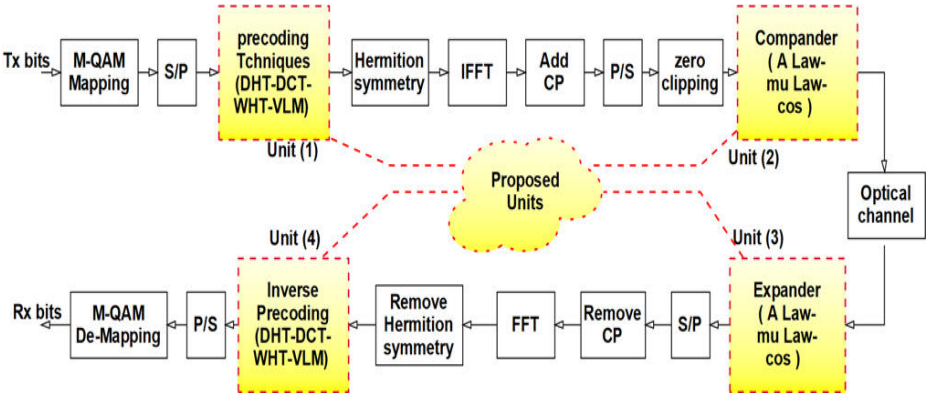

Fig. 2. Proposed combined precoding and companding techniques for the ACO-OFDM-based VLC system.

According to the novelty points addressed in section 1, it is noteworthy to mention that exploring the effect of applying types of the NCT on the PAPR and BER performance in a VLC based system will use units 2 and 3. This will be carried out in section 4 - as previously mentioned. Section 4.1 describes the performance of both BER and PAPR using PCT only with units 1 and 4. The four units will be used to explore the implementation of NCT combined with PCT, as will be presented in section 4.3. A comparison between the NCT, PCT, and a merge between them will be presented in section 4.4.

4. Simulation results

The following sections will use the following parameters used in the available related kinds of literature (i.e., RF and VLC) [20,32,38,50,54–56,58]. Modulation order that uses = 16-QAM symbols. M = 256 and N = 1024 points IFFT are assumed for the number of subcarriers. The PAPR reduction effectiveness is calculated using the PAPR CCDF.

Similar to the previous kind of literature and for comparing purposes, the values of $PAPR_0$ is calculated at CCDF = 10^{-3} to be 17.2 dB for a conventional ACO-OFDM. A key evaluating parameter is the PAPR reduction value (i.e., will be presented in detail in section 4.4 Table 1) which is calculated as the difference between the conventional ACO-OFDM $PAPR_0$ (i.e., 17.2 dB) and the $PAPR_0$ for the technique used. The higher the PAPR reduction value, the better the technique used. This is the main target for this work.

Another evaluating factor is $E_b/N_{0\ diff}$. It is defined as the difference between the E_b/N_0 for the technique under evaluation and the E_b/N_0 for a conventional ACO-OFDM (i.e. 13.5 dB) at BER = 10^{-3}. The factor of $E_b/N_{0\ diff}$ estimates whether the tested technique needs more or less power to achieve the target BER (i.e., = 10^{-3}) compared to the conventional ACO-OFDM. The higher the $E_b/N_{0\ diff}$ with values greater than zero, this means that more power is needed to achieve the targeted BER (i.e., = 10^{-3}) compared to the conventional ACO-OFDM and, hence, lousy performance. On the other hand, the lower this value under zero, the better performance. This will be the basic idea of evaluating the BER performance in the following sections, especially 4.4 (Table 1).

4.1 *Exploring PAPR and BER for NCT*

As indicated previously, this section presents the evaluation of PAPR and BER performance when applying NCT only on ACO-OFDM-based VLC systems with the aforementioned parameters. Again, this analysis uses in Fig. 2 only units 2 and 3.

Figure 3 explores the PAPR performance when applying NCT to the proposed VLC system (i.e., Fig. 2). The figure also contains the performance of the conventional ACO-OFDM (i.e., Fig. 1) for comparison purposes. In the A-law companding technique, the companding factor (A) varies by values 2, 3, 5, 10, and 15. At CCDF = 10^{-3}, when A = 2, 3, 5, 10, and 15, the value of $PAPR_0$ equals 16.22, 14.1, 12.04, 10.54, and 9.617 dB, respectively. This means that the A-law companding technique causes the reduction of the PAPR parameter compared to a conventional ACO-OFDM by increasing A. The value of reduction for different values of A-parameters equals 0.98, 3.1, 5.16, 6.66, and 7.583, respectively.

In the μ-law companding technique, the companding factor (μ) is set to vary by values 2, 3, 5, 10, and 15. At CCD F = 10^{-3}, when μ = 2, 3, 5, 10, and 15, the value of $PAPR_0$ equals 14.45, 13.5, 12, 11.23, and 10.9 dB, respectively. The value of reduction for different values of μ-parameters equals 2.75, 3.7, 5.2, 5.97, and 6.3 dB, respectively. Finally, when the companding factor of cos technique (y) equals 1, the value of $PAPR_0$ decreases to 11.3 dB. Therefore, the value of the PAPR reduction is 5.9 dB compared to a conventional ACO-OFDM.

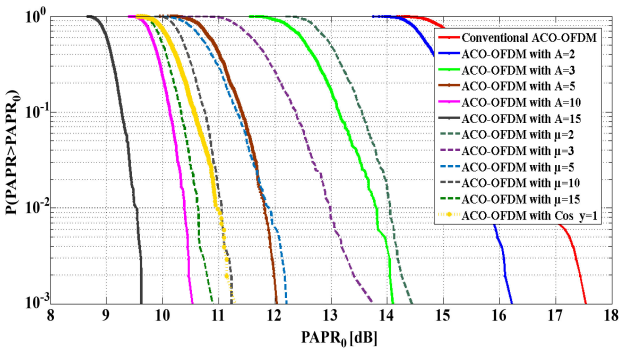

Fig. 3. PAPR comparison between A-law, μ-law, and cos companding techniques for the ACO-OFDM-based VLC system.

Figure 4 explores the BER performance when applying NCT to the proposed VLC system (i.e., Fig. 2). The figure also contains the performance of a conventional ACO-OFDM (i.e., Fig. 1) for comparison purposes. At BER = 10^{-3}, the value of E_b/N_0 for a conventional ACO-OFDM equals 13.5 dB. When applying A-law companding, BER is not changed for the companding factor A equalling 2, 3, and 5. For A equalling 10 and 15, the required E_b/N_0 to achieve BER = 10^{-3} are 14.9 and 15.8 dB, respectively. This means that more power is needed (worse BER performance) by 1.4 and 2.3 dB, respectively to achieve a target BER compared to a conventional ACO-OFDM.

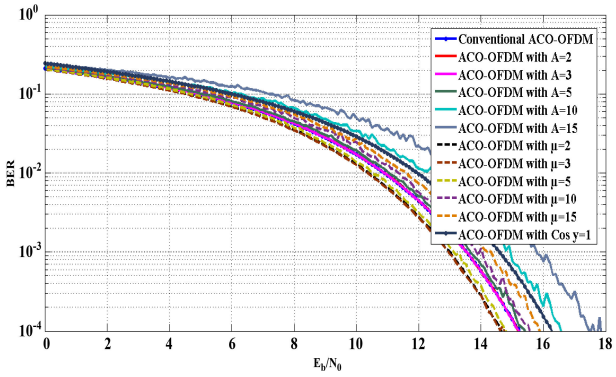

Fig. 4. BER comparison between A-law, μ-law, and cos companding techniques for the ACO-OFDM-based VLC system.

When applying μ -law companding, BER decreases for the companding factor μ equalling 2, 3, and 5. For μ equalling 10 and 15, the required E_b/N_0 to achieve BER = 10^{-3} are 13.8 and 14.2 dB, respectively. Thus, the values of E_b/N_0 increse compared to a conventional ACO-OFDM by 0.3 and 0.7 dB. For cos companding techniques E_b/N_0 increases to 14.6 dB to achieve BER = 10^{-3}. Thus, the values of E_b/N_0 increase compared to a conventional ACO-OFDM by 1.1 dB.

It can be concluded that when applying NCT only to the proposed system, applying only the cos companding technique is considered the worst technique to decrease the PAPR. Also, it requires a higher power (E_b/N_0) to achieve the targeted BER (10^{-3}). It is noted that the A-law companding technique overcomes the performance of μ-law companding techniques at a high value of the companding factor (10, 15) for the PAPR reduction performance. This observation is reversed for the BER performance at the same high value of the companding factor (10, 15).

At the low compounding factor (2, 3, and 5), A-law companding techniques show an attractive performance by reducing the PAPR while not altering the BER behavior. At these values, the PAPR reduction performance is close between A-Law and μ-law companding techniques. Finally, the BER performance of the μ-law companding shows a slight enhancement compared to the A-law.

4.2 *Exploring PAPR and BER for PCT*

As indicated previously, this section used units 1 and 4 only in Fig. 2. This section presents the evaluation of the PAPR and BER performance when applying PCT only on the ACO-OFDM-based VLC systems with the aforementioned parameters.

Figure 5 explores the PAPR performance when applying PCT to the proposed VLC system (i.e., Fig. 2). The figure also contains the performance of a conventional ACO-OFDM (i.e. Fig. 1) for comparison purposes. The value of PAPR0 at CCDF = 10^{-3} for conventional ACO-OFDM, WHT, DCT, DHT, and VLM equals 17.2, 16, 15, 14.5, and 13.6 dB, respectively. Thus, the value of reducing different precoding techniques equals 1.2, 2.2, 2.7, and 3.6 dB. The results show that VLM is an effective type of PCT to overcome the PAPR problem. On the other hand, the BER performance for different PCT types shows a very close performance, as shown in Fig. 6. This is because of the procedure that is followed to reduce PAPR in these techniques.

4.3 *Exploring PAPR and BER for combined PCT and NCT*

As indicated previously, this section presents the evaluation of the PAPR and BER performance when applying PCT combined with NCT on the ACO-OFDM-based VLC system. This analysis used all proposed units (i.e., from 1 to 4) presented in Fig. 2. The scenario of the combination was established by selecting one of the PCTs with all types of NCTs. There are four types of combinations named by DCT with NCT, WHT with NCT, DHT with NCT, and VLM with NCT. The analysis of these four types occurs in the following sections (i.e., 4.3.1 to 4.3.4).

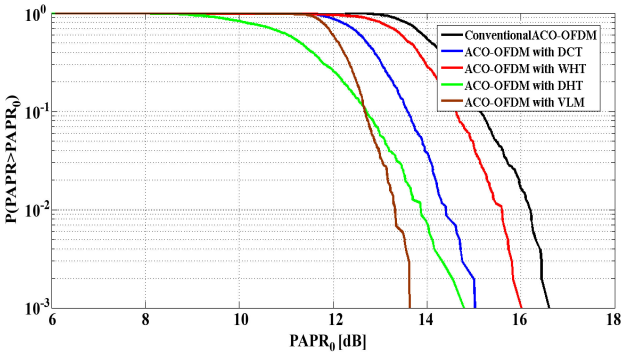

Fig. 5. PAPR comparison between DCT, WHT, DHT, and VLM precoding techniques for the ACO-OFDM-based VLC system.

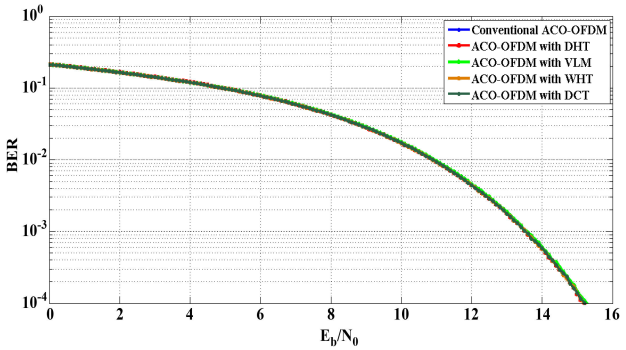

Fig. 6. BER comparison between DCT, WHT, DHT, and VLM precoding techniques for the ACO-OFDM-based VLC system.

4.3.1 A combination of DCT with NCT

The first analysis is done to explore the performance of the combination of DCT with A-law, μ-law, and cos companding techniques. They are shown in Figs. 7 and 8 for PAPR and BER, respectively. In DCT combined with A-law companding techniques, the companding factor (A) is set to vary by values 2, 3, 5, and 10. At CCDF = 10^{-3}, when A = 2, 3, 5, and 10, the value of $PAPR_0$ equals 14.23, 13, 11.22, and 9.548 dB respectively. Therefore, the reduction value for different values of A-factors equals 2.97, 4.2, 5.98, and 7.652 dB.

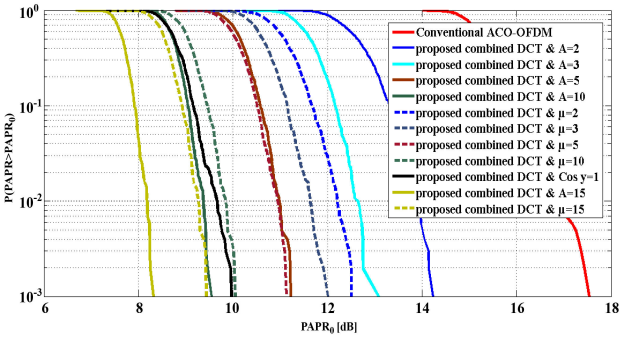

Fig. 7. PAPR compression for the ACO-OFDM system for A-law, μ-law, and cos companding combined with DCT.

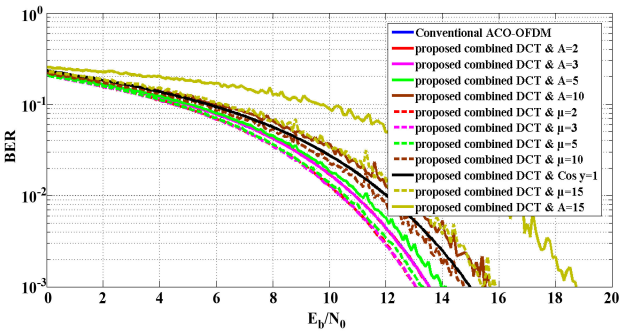

Fig. 8. BER comparison for the ACO-OFDM system for A-law, μ-law, and cos companding combined with DCT.

In DCT combined with μ-law, the companding factor (μ) is set to vary by values 2, 3, 5, and 10. At CCDF = 10^{-3}, when μ = 2, 3, 5, and 10, the value of $PAPR_0$ equals 12.5, 12.01, 11.13, and 10.05 dB, respectively. The reduction value for different values of μ -parameters equals 4.7, 5.19, 6.07, and 7.15 dB, respectively. When the companding factor of cos techniques y is set by 1, the value of $PAPR_0$ decreases to 9.967 dB. Therefore, the value of PAPR reduction is 7.213 dB compared to a conventional ACO-OFDM.

In conclusion, for the low value of the companding factor, the μ-law is better than A-law combined with DCT. However, for A and μ factors greater than 5, the A-law and Cos companding techniques are more effective in PAPR reduction for the proposed system.

Figure 8 shows the BER performance of the combined DCT with NCT. At BER = 10^{-3}, the value of E_b/N_0 for a conventional ACO-OFDM is equal to 13.5 dB. For the companding factor, A equals 2 and 3, the A-law combined with DCT shows a close behavior. For A equalling 5 and 10, the required E_b/N_0 to achieve BER = 10^{-3} are 13.9 and 15.5 dB, respectively. Thus, the values of E_b/N_0 increase compared to a conventional ACO-OFDM by 0.4 and 2 dB, respectively.

BER is enhanced by increasing the companding factor (μ) from 2 to 5 for μ-law combined with DCT. For μ equalling 10, 15, the required E_b/N_0 to achieve BER = 10^{-3} are 14.7 and 15 dB, respectively. This means that we need more power (worse BER performance) by 1.2 and 1.5 dB, respectively, to achieve target BER compared to a conventional ACO-OFDM. For the combined DCT with Cos companding techniques, E_b/N_0 increased to 14.9 dB to achieve BER = 10^{-3}. This means that more power is needed (worse BER performance) by 1.4 dB to achieve a target BER compared to a conventional ACO-OFDM. For cos combined with DCT, its BER performance is better than (A-law or μ-law combined with DCT) at high companding factors, while its performance worsens when A or μ have low companding factor values.

For this part, one can conclude that, for BER analysis, at low companding factors 2 to 5 (A-law or μ-law combined with DCT), the performance is better than high ones (5, 10), and this may be considered as the optimum in all cases. Also, at a low companding factor, the BER performance of μ-law combined with DCT is better but close to the BER performance of A-law combined with DCT.

4.3.2 A combination of WHT with NCT

Starting from this section and to avoid duplication and repetition, the detailed data and discussion previously presented in sections 4.1, 4.2, and 4.3.1 will be abbreviated greatly depending on Table 1 in section 4.4 and the following figures. Only the performance and differences between merged techniques will be evaluated.

Now and as extracted from Table 1 and Fig. 9, the PAPR performance is analyzed when NCT merged with WHT, at low companding factor (i.e., A and μ from 2 to 5). μ-law combined with WHT shows the optimum possible PAPR reduction among all merging NCT with WHT. A-law combined with WHT achieves the optimum possible performance at a high companding factor (i.e., A and $\mu > 5$).

Figure 10 and data extracted from Table 1 lead to the observation that the BER performance for A-law and μ-law combined with WHT are quite similar at low companding factor (i.e., A and μ from 2 to 5) with attractive characteristics. μ-law at higher companding factors and cos combined with WHT overcomes the performance of A-law combined with WHT. Finally, μ-law combined with WHT

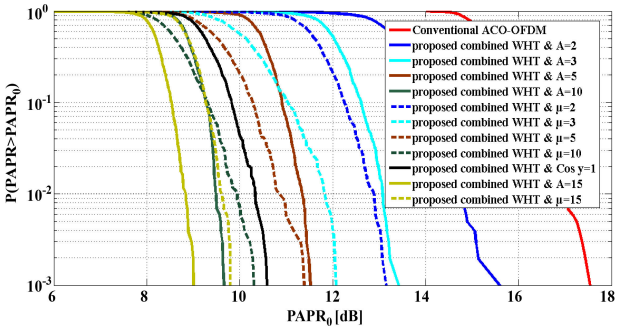

Fig. 9. PAPR compression for the ACO-OFDM system for A-law, μ-law, and cos companding combined with WHT.

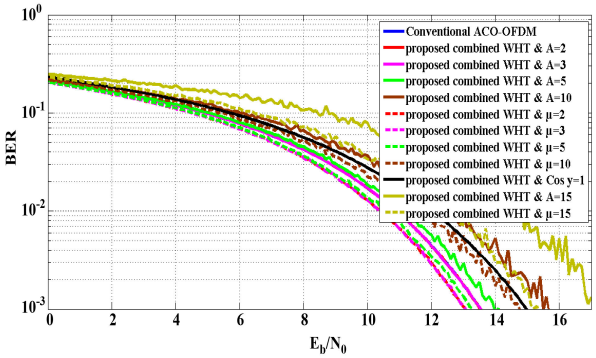

Fig. 10. BER comparison for the ACO-OFDM system for A-law, μ-law, and cos companding combined with WHT.

can be considered the optimum solution for the BER performance and power requirement.

4.3.3 *A combination of DHT with NCT*

From Table 1 and Figs. 11 and 12, the PAPR performance is obtained when NCT is merged with DHT, at low companding factor (i.e., A and μ from 2 to 5). μ-law combined with DHT shows the optimum possible PAPR reduction among all merging NCT with DHT. A-law combined with DHT achieves the optimum possible performance at a high companding factor (i.e., A and $\mu > 5$). This conclusion shows a great matching with that obtained for the corresponding WHT merged with NCT. More details will be addressed in section 4.4.

4.3.4 *A combination of VLM with NCT*

The fourth proposed combined techniques between VLM precoding techniques with A-law, μ-law, and cos companding techniques are shown in Figs. 13 and 14 for the PAPR and BER performance, respectively. Table 1 and these figures lead to the same general behavior observed and concluded in sections 4.3.2 and 4.3.3. The difference taking place in the values is clearly illustrated in Table 1. The comparison and ordering techniques will be presented in the following section.

4.4 *Comparison between NCT, PCT and merging between them*

In this section, a numerical comparison between NCT, PCT and merging between them extracted from Figs. 3 to 14 is carried out in Table 1. Similar to previous kinds of literature and for comparing purposes, the values of $PAPR_0$ and E_b/N_0 are extracted at CCDF = 10^{-3} and BER = 10^{-3} respectively, where $PAPR_0$ = 17.2 dB, E_b/N_0 = 13.5 dB for a conventional ACO-OFDM. PAPR reduction value and the required $E_b/N_{0\ diff}$ are used as evaluating parameters and are presented in Table 1.

First, when observing the PAPR performance (i.e., PAPR reduction value) of NCT alone or PCT alone, it can be found that merging techniques generally outcome their performance. Since PAPR is the main interest of this work, the following discussion will focus only on the merging techniques perfomance.

- For the merging between A-law companding with PCT, it is observed that:
  1. At companding factors from 2 to 10, the optimum PAPR performance is ordered as merging with VLM, then DHT, then DCT, and finally WHT.
  2. At companding factors greater than 10, the optimum PAPR performance is ordered as merging with VLM, then DCT, then DHT, and finally WHT.

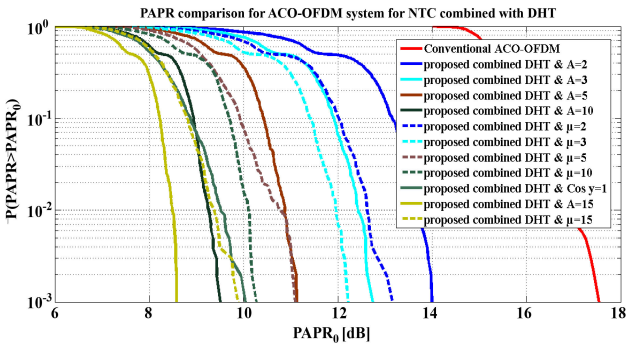

Fig. 11. PAPR comparison for ACO-OFDM system for A-law, μ-law, and cos companding combined with DHT.

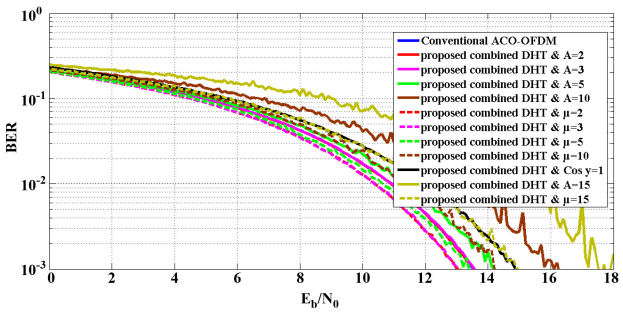

Fig. 12. BER comparison for the ACO-OFDM system for A-law, μ-law, and cos companding combined with DHT..

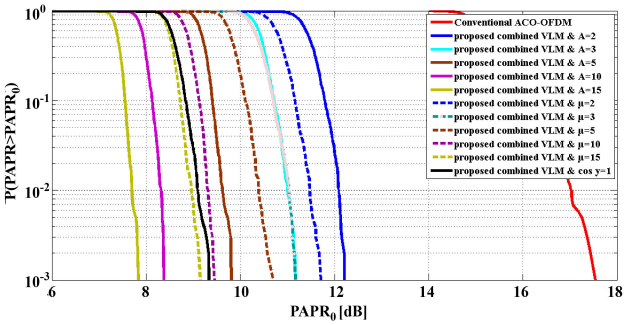

Fig. 13. PAPR comparison for the ACO-OFDM system for A-law, μ-law, and cos companding combined with VLM.

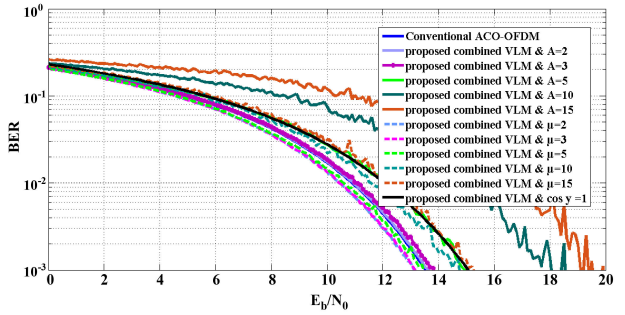

Fig. 14. BER comparison for the ACO-OFDM system for A-law, μ-law, and cos companding combined with VLM.

Table 1.
$PAPR_0$ and E_b/N_0 values at CCDF=10^{-3}& BER=10^{-3}. PAPR reduction value and required E_b/N_0 to achieve the same BER w.r.t. conventional ACO-OFDM, where $PAPR_0$=17.2dB, E_b/N_0 =13.5dB for ACO-OFDM

							PCT													
							DCT				DHT				WHT				VLM			
		Companding factor	$PAPR_0$	PAPR reduction	E_b/N_0 for NCT	E_b/N_0 *diff*	$PAPR_0$	PAPR reduction	E_b/N_0	E_b/N_0 *diff*	$PAPR_0$	PAPR reduction	E_b/N_0	E_b/N_0 *diff*	$PAPR_0$	PAPR reduction	E_b/N_0	E_b/N_0 *diff*	$PAPR_0$	PAPR reduction	E_b/N_0	E_b/N_0 *diff*
$PAPR_0$ for PCT							15	2.2	13.5	0	14.5	2.7	13.5	0	16	1.2	13.5	0	13.6	3.6	13.5	0
NCT	A-Law	2	16.22	0.98	13.5	0	14.23	2.97	13.5	0	13.99	3.21	13.5	0	15.6	1.6	13.5	0	12.1	5.1	13.5	0
		3	14.1	3.1	13.5	0	13	4.2	13.5	0	12.74	4.46	13.5	0	13.43	3.77	13.5	0	10.96	6.24	13.9	0.4
		5	12.04	5.16	13.6	0.1	11.22	5.98	13.9	0.4	11.13	6.07	14.1	0.6	11.52	5.68	13.9	0.4	9.84	7.36	15.1	1.6
		10	10.54	6.66	14.9	1.4	9.548	7.652	15.5	2	9.512	7.688	16.1	2.6	9.66	7.54	15.6	2.1	8.277	8.923	18.2	4.7
		15	9.617	7.583	15.8	2.3	8.325	8.875	18.7	5.2	8.788	8.412	17.4	3.9	9	8.2	17.1	3.6	7.789	9.411	19.1	5.6
	μ-Law	2	14.45	2.75	13	-0.5	12.5	4.7	13	-0.5	13.16	4.04	13	-0.5	13.15	4.05	13	-0.5	11.68	5.52	13.1	-0.4
		3	13.5	3.7	13	-0.5	12.01	5.19	13	-0.5	12.22	4.98	13	-0.5	12.07	5.13	13	-0.5	11.32	5.88	13.1	-0.4
		5	12	5.2	13.1	-0.4	11.13	6.07	13.2	-0.3	11.1	6.1	13.2	-0.3	11.39	5.81	13.2	-0.3	10.57	6.63	13.4	-0.1
		10	11.23	5.97	13.8	0.3	10.05	7.15	14.7	1.2	10.27	6.93	14.2	0.7	10.3	6.9	14.2	0.7	9.564	7.636	14.4	0.9
		15	10.9	6.3	14.2	0.7	9.454	7.746	15	1.5	9.882	7.318	14.9	1.4	9.858	7.342	14.7	1.2	9.1	8.1	14.9	1.4
	cos(y)	1	11.3	5.9	14.6	1.1	9.967	7.233	14.9	1.4	10.04	7.16	14.8	1.3	10.58	6.62	14.6	1.1	9.447	7.753	15	1.5

3. For BER performance and companding factors from 2 to 3, the performance is not altered compared to the conventional ACO-OFDM.
4. For BER performance and companding factors greater than 5, the optimum performance is ordered as merging with WHT/DCT, then DHT, and finally VLM.

- For the merging between μ-law companding with PCT, it is observed that:
  1. At all companding factors, the optimum PAPR performance is ordered as merging with VLM, then DCT, then WHT, and finally DHT.
  2. For BER performance and companding factors ≤ 5, the performance-enhanced compared to conventional ACO-OFDM. The performance of merging with different PCT is close.
  3. For BER performance and companding factors > 5, the performance degraded compared to conventional ACO-OFDM. Merging μ-law companding with WHT/DHT provides the optimum BER performance at this range of companding factors. This is followed by merging with VLM and finally DCT.

- For the merging between cos companding with PCT, it is observed that:
  1. The optimum PAPR performance is ordered as merging with VLM, then DCT, then DHT, and finally WHT.
  2. For BER performance, the optimum performance is ordered as merging with WHT, then DCT/DHT, and finally VLM.

- As conclusion:
  1. When targeting a very high PAPR reduction value regarding BER performance (i.e., lousy BER performance), one can use A-law companding with VLM.
  2. Cos companding can provide an acceptable PAPR reduction value and a reasonable BER performance only when merged with DHT. Its performance in this merging outcomes that observed for μ-law and A-law when merged with DHT.
  3. The optimum merging between all techniques that balance between the highest possible PAPR reduction value and the very acceptable BER performance is μ-law companding merged with VLM at all companding factors. However, an overall PAPR reduction of 8.1 dB can be obtained at $\mu = 15$. Hence, a system accuracy $E_b/N_{0\ diff} = 1.4$ dB can be achieved at a BER perforamnce of 10^{-3}.

5. Comparison with related studies

This section provides a detailed specification comparison between this work and the related literature as presented in Table 2. The key judgment factors definition and the indication of their values are those set with details at the beginning of section 4 and repeated at the start of subsection 4.4.

Table 2 indicates that this work provides a unique advantage of achieving the highest calculated PAPR reduction value set as the main goal for all PAPR reduction-based literature. This is done when choosing VLM combined with μ-law companding techniques from all the techniques discussed through this work. This result is associated with a high IFFT size (i.e., extensive processing data) and an acceptable modulation order. On the other hand, when observing the second lower priority judgment factor ($E_b/N_{0\ diff}$), Table 2 indicates that for VLM combined with μ-law companding techniques a 1.4 dB more power over E_b/N_0 for a conventional ACO-OFDM (i.e., 13.5 dB) is required to achieve the targeted BER (i.e., $= 10^{-3}$). This is not significant (i.e., lower than zero is great) value, remarkable values for this factor can be found in section 4.4 but with a price of a lower PAPR reduction and with other techniques rather than VLM combined with μ-law companding techniques. Still, this value is more than acceptable, especially when associated with the achievement of the PAPR reduction value and the system complexity.

Table 2.
A comparison between the studies and the presented work for different PAPR reduction techniques with ACO-OFDM.

Ref.	System	IFFT Size	Modulation Order	PAPR Reduction Value	$E_b/N_{0\ diff}$
[60]	Clipped ACO-OFDM with clipping mitigatio using (TDCSR/FDCDR [1]	1024	16-QAM	(5.6 dB/ 5.3 dB)	accept-able
[61]	SACO-OFDM/ESACO-OFDM [2]	128	16-QAM 64-QAM 256-QAM	~ (1.2 dB/ 1.4 dB)	1 dB 2 dB 3 dB
[62]	SVT-SLM [3]	512	16-QAM	~ 4.1 dB	NA
[63]	PA-OOFDM [4]	1024	M-QAM	~ 2.2 dB	NA
[50]	WHT-OOFDM DCT-OOFDM DHT-OOFDM VLM-OOFDM	256	16-QAM	0.93 dB 1.89 dB 1.27 dB 2.9 dB	NA
[64]	RoC-ACO-OFDM[5] with MAP [6] -based detection algorithm	256	64-QAM	7.3 dB	4 dB
[65]	the Toeplitz matrix-based Gaussian blur method	256	16-QAM	6 dB	~2 dB
Proposed	VLM combined with μ-law companding techniques	1024	16-QAM	8.1 dB	~1.4 dB

[1]TDCSR/FDCDR – Time-Domain Clipped Sample Reconstruction/Frequency–Domain Clipping Distortion Removal.
[2]SACO-OFDM/ ESACO-OFDM – Subcarrier-index modulation-based ACO-OFDM/Enhanced SACO-OFDM.
[3] SVT-SLM – Symmetric Vector Transformation- Selected Mapping.
[4]PA-OOFDM – Pilot-Assisted Optical OFDM.
[5] RoC-ACO-OFDM – Recoverable Upper Clipping-ACO-OFDM.
[6]MAP – Maximum A Posteriori.

6. Conclusions

This work proposes several PAPR reduction schemes for ACO-OFDM VLC systems. The proposed techniques are tested and compared to each other to nominate an effective scheme that is capable of reducing PAPR as much as possible while maintaining an acceptable BER performance. This work increases the compatibility of ACO-OFDM schemes to practical applications. The proposed μ-law companding technique merged with VLM at the companding factor from 2 to 15 achieves the optimum possible performance. For example, a nominated performance is achieved at $\mu = 15$ with a PAPR reduction value equal to 8.1 dB and the $E_b/N_{0\ diff} = 1.4$ dB. A comparison with related literature is carried out to validate and ensure the novelty of the proposed schemes along with their performance.

REFERENCES

[1] Mohammed, N. A. & Elkarim, M. A. Exploring the effect of diffuse reflection on indoor localization systems based on RSSI-VLC. *Opt. Express* **23**, 20297 (2015), https://doi.org/10.1364/oe.23.020297.

[2] Grobe, L. *et al.* High-speed visible light communication systems. *IEEE Commun. Mag.* **51**, 60–66 (2013), https://doi.org/10.1109/MCOM.2013.6685758.

[3] Mohammed, N. A. & Mansi, A. H. Performance enhancement and capacity enlargement for a DWDM-PON system utilizing an optimized cross seeding rayleigh backscattering design. *Appl. Sci.* **9**, 4520 (2019), https://doi.org/10.3390/app9214520.

[4] Mohammed, A. N., Okasha, M. N. & Aly, M. H. A wideband apodized FBG dispersion compensator in long haul WDM systems. *J. Optoelectron. Adv. Mater.* **18**, 475–479 (2016).

[5] Mohammed, N. A. & El Serafy, H. O. Ultra-sensitive quasi-distributed temperature sensor based on an apodized fiber Bragg grating. *Appl. Opt.* **57**, 273 (2018), https://doi.org/10.1364/ao.57.000273.

[6] Mohammed, N. A. & Okasha, N. M. Single- and dual-band dispersion compensation unit using apodized chirped fiber Bragg grating. *J. Comput. Electron.* **17**, 349–360 (2018), https://doi.org/10.1007/s10825-017-1096-2.

[7] Shehata, M. I. & Mohammed, N. A. Design and optimization of novel two inputs optical logic gates (NOT, AND, OR and NOR) based on single commercial TW-SOA operating at 40 Gbit/s. *Opt. Quantum Electron.* **48**, 1–16 (2016), https://doi.org/10.1007/s11082-016-0602-2.

[8] Mohammed, N. A., Hamed, M. M., Khalaf, A. A. M., Alsayyari, A. & El-Rabaie, S. High-sensitivity ultra-quality factor and remarkable compact blood components biomedical sensor based on nanocavity coupled photonic crystal. *Results Phys.* **14**, 102478 (2019), https://doi.org/10.1016/j.rinp.2019.102478.

[9] Mohammed, N. A., Abo Elnasr, H. S. & Aly, M. Performance evaluation and enhancement of 2×2 Ti: LiNbO 3 Mach Zehnder interferometer switch at 1.3 µm and 1.55 µm. *Open Electr. Electron. Eng. J.* **6**, 36–49 (2012), https://doi:10.2174/1874129001206010036

[10] Mostafa, T. S., Mohammed, N. A. & El-Rabaie, E. S. M. Ultra-h igh bit rate all-optical AND/OR logic gates based on photonic crystal with multi-wavelength simultaneous operation. *J. Mod. Opt.* **66**, 1005–1016 (2019), https://doi.org/10.1080/09500340.2019.1598587.

[11] Mohammed, N. A., Abo Elnasr, H. S. & Aly, M. H. Analysis and design of an electro-optic 2 × 2 switch using Ti: KNbO3 as a waveguide based on MZI at 1.3 µ m. *Opt. Quantum Electron.* **46**, 295–304 (2014), https://doi.org/10.1007/s11082-013-9760-7.

[12] Mostafa, T. S., Mohammed, N. A. & El-Rabaie, E. S. M. Ultracompact ultrafast-switching-speed all-optical 4×2 encoder based on photonic crystal. *J. Comput. Electron.* **18**, 279–292 (2019), https://doi.org/10.1007/s10825-018-1278-6.

[13] Jovicic, A., Li, J. & Richardson, T. Visible light communication: opportunities, challenges and the path to market. *IEEE Commun. Mag.* **51**, 26–32 (2013).

[14] Rehman, S. U., Ullah, S., Chong, P. H. J., Yongchareon, S. & Komosny, D. Visible light communication: A system perspective–Overview and challenges. *Sensors* **19**, 1153 (2019), https://doi.org/10.3390/s19051153.

[15] Matheus, L. E. M., Vieira, A. B., Vieira, L. F. M., Vieira, M. A. M. & Gnawali, O. Visible light communication: concepts, applications and challenges. *IEEE Commun. Surv. Tutorials* **21**, 3204 (2019), https://doi.org/10.1109/COMST.2019.2913348.

[16] Rust, I. C. & Asada, H. H. A dual-use visible light approach to integrated communication and localization of underwater robots with application to non-destructive nuclear reactor inspection. In *IEEE International Conference on Robotics Automation (ICRA2012)* 2445–2450 (2012), https://doi.org/10.1109/ICRA.2012.6224718.

[17] Mohammed, N. A., Badawi, K. A., Khalaf, A. A. M. & El-Rabaie, S. Dimming control schemes combining IEEE 802.15.7 and SC-LPPM modulation schemes with an adaptive M-QAM OFDM for indoor LOS VLC systems. *Opto-Electron. Rev.* **28**, 203–212 (2020), https://doi.org/10.24425/opelre.2020.135259.

[18] Mohammed, N. A. & Badawi, K. A. Design and performance evaluation for a non-line of sight VLC dimmable system based on SC-LPPM. *IEEE Access* **6**, 52393–52405 (2018), https://doi.org/10.1109/ACCESS.2018.2869878.

[19] Shoreh, M.H., Fallahpour, A. & Salehi, J.A. Design concepts and performance analysis of multicarrier CDMA for indoor visible light communications. *J. Opt. Commun. Netw.* **7**, 554–562 (2015), https://doi.org/10.1364/JOCN.7.000554.

[20] Mossaad, M. S. A., Hranilovic, S. & Lampe, L. Visible light communications using OFDM and multiple LEDs. *IEEE Trans. Commun.* **63**, 4304–4313 (2015), https://doi.org/10.1109/TCOMM.2015.2469285.

[21] Badawi, K. A., Mohammed, N. A. & Aly, M. H. Exploring BER performance of a SC-LPPM based LOS-VLC system with distinctive lighting. *J. Optoelectron. Adv. Mater.* **20**, 290–301 (2018).

[22] Mohammed, N. A, Abaza, M. R. & Aly, M. H. Improved performance of M-ary PPM in different free-space optical channels due to reed solomon code using APD. *J. Sci. Eng. Res.* **2**, 82–85 (2011).

[23] Tsonev, D., Sinanovic, S. & Haas, H. Novel unipolar orthogonal frequency division multiplexing (U-OFDM) for optical wireless. in *IEEE Vehicular Technology Conference* (2012), https://doi.org/10.1109/VETECS.2012.6240060.

[24] Islam, R., Choudhury, P. & Islam, M. A. Analysis of DCO-OFDM and flip-OFDM for IM/DD optical-wireless system. in *8th International Confference on Electrical and Computer Engineering: Advancing Technology for a Better Tomorrow (ICECE 2014)* 32–35 (2015), https://doi.org/10.1109/ICECE.2014.7026929.

[25] Hu, W. W. PAPR reduction in DCO-OFDM visible light communication systems using optimized odd and even sequences combination. *IEEE Photonics J.* **11**, 1024 (2019), https://doi.org/10.1109/JPHOT.2019.2892871.

[26] Dissanayake, S. D., Panta, K. & Armstrong, J. A novel technique to simultaneously transmit ACO-OFDM and DCO-OFDM in IM/DD systems. in *IEEE Globecom Workshops (GC Wkshps 2011)* 782–786 (2011), https://doi.org/10.1109/GLOCOMW.2011.6162561.

[27] Dissanayake, S. D., Member, S., Armstrong, J. & Member, S. Comparison of ACO-OFDM, DCO-OFDM and ADO-OFDM in IM/DD Systems. *J. Light. Technol.* **31**, 1063–1072 (2013).

[28] Dang, J., Zhang, Z. & Wu, L. Improving the power efficiency of enhanced unipolar OFDM for optical wireless communication. *Electron. Lett.* **51**, 1681–1683 (2015), https://doi.org/10.1049/el.2015.2024.

[29] Lam, E., Wilson, S. K., Elgala, H. & Little, T. D. C. Spectrally and energy efficient OFDM (SEE-OFDM) for intensity modulated optical wireless systems. The Cornell University,1–26 (2015), https://arxiv.org/abs/1510.08172v1

[30] Lowery, A. J. Comparisons of spectrally-enhanced asymmetrically-clipped optical OFDM systems. *Opt. Express* **24**, 3950 (2016), https://doi.org/10.1364/oe.24.003950.

[31] Elgala, H. & Little, T. Polar-based OFDM and SC-FDE links toward energy-efficient Gbps transmission under IM-DD optical system constraints. *J. Opt. Commun. Netw.* **7**, A277–A284 (2015), https://doi.org/10.1364/JOCN.7.00A277.

[32] Zhang, T. *et al.* A performance improvement and cost-efficient ACO-OFDM scheme for visible light communications. *Opt. Commun.* **402**, 199–205 (2017), https://doi.org/10.1016/j.optcom.2017.06.015.

[33] Kubjana, M. D., Shongwe, T. & Ndjiongue, A. R. Hybrid PLC-VLC based on ACO-OFDM. in *2018 IEEE International Conference On Intelligent And Innovative Computing Applications (ICONIC 2018)*

364–368 (2018).

[34] Shawky, E., El-Shimy, M. A., Shalaby, H. M. H., Mokhtar, A. & El-Badawy, E.-S. A. Kalman Filtering for VLC Channel Estimation of ACO-OFDM Systems. in *2018 ASIA IEEE Communications And Photonics Conference (ACP)* (2018).

[35] Niaz, M. T., Imdad, F., Ejaz, W. & Kim, H. S. Compressed sensing-based channel estimation for ACO-OFDM visible light communications in 5G systems. *Eurasip J. Wirel. Commun. Netw.* **2016**, 268 (2016). https://doi.org/10.1186/s13638-016-0774-2.

[36] Hao, L., Wang, D., Cheng, W., Li, J. & Ma, A. Performance enhancement of ACO-OFDM-based VLC systems using a hybrid autoencoder scheme. *Opt. Commun.* **442**, 110–116 (2019), https://doi.org/10.1016/j.optcom.2019.03.013.

[37] Vappangi, S. & Vakamulla, V. M. Channel estimation in ACO-OFDM employing different transforms for VLC. *AEU-Int. J. Electron. Commun.* **84**, 111–122 (2018), https://doi.org/10.1016/j.aeue.2017.11.016.

[38] Vappangi, S. & Vakamulla, V. M. A low PAPR multicarrier and multiple access schemes for VLC. *Opt. Commun.* **425**, 121–132 (2018), https://doi.org/10.1016/j.optcom.2018.04.064.

[39] Mounir, M., Tarrad, I. F. & Youssef, M. I. Performance evaluation of different precoding matrices for PAPR reduction in OFDM systems. *Internet Technol. Lett.* **1**, e70 (2018), https://doi.org/10.1002/itl2.70.

[40] Hu, S., Wu, G., Wen, Q., Xiao, Y. & Li, S. Nonlinearity reduction by tone reservation with null subcarriers for WiMAX system. *Wirel. Pers. Commun.* **54**, 289–305 (2010), https://doi.org/10.1007/s11277-009-9726-z.

[41] Zhang, X., Wang, Q., Zhang, R., Chen, S. & Hanzo, L. Performance analysis of layered ACO-OFDM. *IEEE Access* **5**, 18366–18381 (2017), https://doi.org/10.1109/ACCESS.2017.2748057.

[42] Anoh, K., Tanriover, C., Adebisi, B. & Hammoudeh, M. A new approach to iterative clipping and filtering papr reduction scheme for ofdm systems. *IEEE Access* **6**, 17533–17544 (2017), https://doi.org/10.1109/ACCESS.2017.2751620.

[43] Madhavi, D. & Ramesh Patnaik, M. Implementation of non linear companding technique for reducing PAPR of OFDM. *Mater. Today Proc.* **5**, 870–877 (2018), https://doi.org/10.1016/j.matpr.2017.11.159.

[44] Shaheen, I. A. A., Zekry, A., Newagy, F. & Ibrahim, R. Absolute exponential companding to reduced PAPR for FBMC/OQAM. in *2017 Palestinian International Confference on Information and Communication Technology* (*PICICT 2017*) 60–65 (2017), https://doi.org/10.1109/PICICT.2017.17.

[45] Yang, Y., Zeng, Z., Feng, S. & Guo, C. A simple OFDM scheme for VLC systems based on μ-law mapping. *IEEE Photonics Technol. Lett.* **28**, 641–644 (2016), https://doi.org/10.1109/LPT.2015.2503481.

[46] Yadav, A.K. & Prajapati, Y. K. PAPR minimization of clipped ofdm signals using tangent rooting companding technique. *Wirel. Pers. Commun.* **105**, 1435–1447 (2019), https://doi.org/10.1007/s11277-019-06151-1.

[47] Hasan, M. M. VLM precoded SLM technique for PAPR reduction in OFDM systems. *Wirel. Pers. Commun.* **73**, 791–801 (2013), https://doi.org/10.1007/s11277-013-1217-6.

[48] Freag, H. *et al*. PAPR reduction in VLC-OFDM system using CPM combined with PTS method. *Int. J. Comput. Digit. Syst.* **6**, 127–132 (2017), https://doi.org/10.12785/ijcds/060304.

[49] Xiao, Y. *et al.* PAPR reduction based on chaos combined with SLM technique in optical OFDM IM/DD system. *Opt. Fiber Technol.* **21**, 81–86 (2015), https://doi.org/10.1016/j.yofte.2014.08.014.

[50] Wang, Z., Wang, Z. & Chen, S. Encrypted image transmission in OFDM-based VLC systems using symbol scrambling and chaotic DFT precoding. *Opt. Commun.* **431**, 229–237 (2019), https://doi.org/10.1016/j.optcom.2018.09.045.

[51] Sharifi, A. A. PAPR reduction of optical OFDM signals in visible light communications. *ICT Express* **5**, 202–205 (2019), https://doi.org/10.1016/j.icte.2019.01.001.

[52] Ghassemlooy, Z., Ma, C. & Guo, S. PAPR reduction scheme for ACO-OFDM based visible light communication systems. *Opt. Commun.* **383**, 75–80 (2017), https://doi.org/10.1016/j.optcom.2016.07.073

[53] Abd Elkarim, M., Elsherbini, M. M., AbdelKader, H. M. & Aly, M. H. Exploring the effect of LED nonlinearity on the performance of layered ACO-OFDM. *Appl. Opt.* **59**, 7343–7351 (2020), https://doi.org/10.1364/AO.397559

[54] Kumar Singh, V. & Dalal, U. D. Abatement of PAPR for ACO-OFDM deployed in VLC systems by frequency modulation of the baseband signal forming a constant envelope. *Opt. Commun.* **393**, 258–266 (2017), https://doi.org/10.1016/j.optcom.2017.02.065.

[55] Wang, Z.-P., Xiao, J.-N., Li, F. & Chen, L. Hadamard precoding for PAPR reduction in optical direct detection OFDM systems. *Optoelectron. Lett.* **7**, 363–366 (2011), https://doi.org/10.1007/s11801-011-1044-5.

[56] Wang, Z.-P. & Zhang, S.-Z. Grouped DCT precoding for PAPR reduction in optical direct detection OFDM systems. *Optoelectron. Lett.* **9**, 213–216 (2013), https://doi.org/10.1007/s11801-013-3021-7.

[57] Ali Sharifi, A. Discrete Hartley matrix transform precoding-based OFDM system to reduce the high PAPR. *ICT Express* **5**, 100–103 (2019), https://doi.org/10.1016/j.icte.2018.07.001.

[58] El-Nabawy, M. M., Aboul-Dahab, M. A. & El-Barbary, K. PAPR Reduction of OFDM signal by using combined hadamard and modified meu-law companding techniques. *Int. J. Comput. Networks Commun.* **6**, 71 (2014).

[59] Reddy, Y. S., Reddy, M. V. K., Ayyanna, K. & Ravikumar, G. V. The effect of NCT techniques on SC-FDMA system in presence of HPA. *Int. J. Res. Computer Commun. Technol*. **3**, 844–848 (2014).

[60] Abd El-Rahman, A. F. *et al.* Companding techniques for SC-FDMA and sensor network applications. *Int. J. Electron. Lett.* **8**, 241–255 (2020), https://doi.org/10.1080/21681724.2019.1600051.

[61] Azim, A. W., Le Guennec, Y. & Maury, G. Decision-directed iterative methods for PAPR reduction in optical wireless OFDM systems. *Opt. Commun.* **389**, 318–330 (2017), https://doi.org/10.1016/j.optcom.2016.12.026.

[62] Guan, R. *et al.* Enhanced subcarrier-index modulation-based asymmetrically clipped optical OFDM using even subcarriers. *Opt. Commun.* **402**, 600–605 (2017), https://doi.org/10.1016/j.optcom.2017.06.032.

[63] Hu, W. W. SLM-based ACO-OFDM VLC system with low-complexity minimum amplitude difference decoder. *Electron. Lett.* **54**, 144–146 (2018), https://doi.org/10.1049/el.2017.3158.

[64] Offiong, F. B., Sinanovic, S. & Popoola, W. O. On PAPR reduction in pilot-assisted optical OFDM communication systems. *IEEE Access* **5**, 8916–8929 (2017), https://doi.org/10.1109/ACCESS.2017.2700877.

[65] Xu, W., Wu, M., Zhang, H., You, X. & Zhao, C. ACO-OFDM-specified recoverable upper clipping with efficient detection for optical wireless communications. *IEEE Photonics J.* **6**, (2014), https://doi.org/10.1109/JPHOT.2014.2352643.